

Review of capabilities of multi-angle and polarization cloud measurements from POLDER

F. Parol ^{a,*}, J.C. Buriez ^a, C. Vanbauce ^a, J. Riedi ^a, L. C.-Labonnote ^a,
M. Doutriaux-Boucher ^a, M. Vesperini ^a, G. Sèze ^b,
P. Couvert ^c, M. Viollier ^d, F.M. Bréon ^c

^a Laboratoire d'Optique Atmosphérique, Université des Sciences et Technologies de Lille, 59655 Villeneuve d'Ascq Cedex, France

^b Laboratoire de Météorologie Dynamique, CNRS, Université Pierre et Marie Curie, 75252 Paris Cedex 05, France

^c Laboratoire des Sciences du Climat et de l'Environnement, Commissariat à l'Energie Atomique, 91191 Gif sur Yvette, France

^d Laboratoire de Météorologie Dynamique, CNRS, Ecole Polytechnique, 91128 Palaiseau Cedex, France

Received 28 November 2002; received in revised form 29 January 2003; accepted 29 January 2003

Abstract

Polarization and directionality of the Earth's reflectances (POLDER) is a multispectral imaging radiometer–polarimeter with a wide field-of-view, a moderate spatial resolution, and a multi-angle viewing capability. It functioned nominally aboard ADEOS1 from November 1996 to June 1997. When the satellite passes over a target, POLDER allows to observe it under up to 14 different viewing directions and in several narrow spectral bands of the visible and near-infrared spectrum (443–910 nm). This new type of multi-angle instruments offers new opportunity for deriving cloud parameters at global scale. The aim of this short overview paper is to point out the main contributions of such an instrument for cloud study through its original instrumental capabilities (multi-directionality, multipolarization, and multispectrality). This is mainly illustrated by using ADEOS 1-POLDER derived cloud parameters which are operationally processed by CNES and are available since the beginning of 1999.

© 2003 COSPAR. Published by Elsevier Ltd. All rights reserved.

1. Introduction

As a component of the new generation of Earth-orbiting instruments designed for Earth's observation, the POLDER (polarization and directionality of the Earth's reflectances) is a CNES (the French Space Agency) instrument on board the Japanese Advanced Earth Observing Satellite (ADEOS) launched in August 1996. It worked perfectly until ADEOS's early end of service on June 30, 1997.

The POLDER levels 2 and 3 products routinely processed by CNES are split into three processing lines: "Earth radiation budget, water vapor and clouds" (hereafter "ERB & clouds"), "Ocean color and aerosols over ocean", "Land surfaces and aerosols over land". An overview of algorithms and products of the "ERB &

clouds" line is presented in Buriez et al. (1997). First analysis of POLDER data and validation activity are presented in Parol et al. (1999). The aim of this overview paper is to point out the main contributions of POLDER for cloud studies at global scale and to demonstrate how POLDER's unique instrument capabilities (multidirectionality, multipolarization, and multispectrality) can be used to gain new insights on clouds and the Earth's radiation budget. This new type of multi-angle instrument offers new opportunity for deriving cloud parameters at global scale. This is mainly illustrated by using ADEOS 1-POLDER derived cloud parameters which are operationally processed by CNES and are available since the beginning of 1999.

Without a doubt, the most original characteristics of POLDER is its ability to measure the polarized component of the Earth-atmosphere reflected light. However, as illustrated here, it clearly appears that multi-angle capability is necessary for taking advantage of polarization. For instance, polarization and

* Corresponding author. Tel.: +33-320-43-43-11; fax: +33-320-43-43-42.

E-mail address: frederic.parol@univ-lille1.fr (F. Parol).

multi-directionality allow for determining cloud thermodynamic phase, which is an important cloud parameter for climate models.

The multi-directional capability of POLDER allows for checking schemes of cloud optical thickness and albedo retrieval. Those cloud properties can be derived from usual bidirectional reflectance measurements. However, this needs some assumptions both on cloud microphysics and on cloud morphology and spatial distribution. While it is always possible to find a cloud model that satisfies one single directional observation of a given cloud target, it is not so easy to fulfill the complete set of ten or more observations provided by multidirectional instruments. Consequently, it is shown that POLDER not only allows for determining cloud optical thickness under some hypotheses, but it also enables us to test the validity of these hypotheses.

Finally, we present recent results of derivation of top-of-the-atmosphere ERB from POLDER. These results are compared to the ERBE (Barkstrom et al., 1989), ScaRaB (Scanner for Radiation Budget) (Kandel et al., 1998) and CERES (Wielicki et al., 1996) records.

2. The polder instrument and data

The first POLDER instrument flew on ADEOS between August 1996 and June 1997. POLDER is a multispectral imaging radiometer–polarimeter composed of a two-dimensional charged coupled device (CCD) detector array, wide field of view (~ 2400 km) telecentric optics and a rotating wheel carrying spectral and polarized filters. The dimension of the CCD detector array (242×274 detectors) provides a moderate spatial resolution (~ 6 km), and a multi-angle viewing capability. When the ADEOS satellite passes over a target, up to 14 different images are acquired in several narrow spectral bands of the visible and near-infrared spectrum (443–910 nm). Full azimuthal angle coverage for viewing zenith angles up to $\sim 60^\circ$ is obtained by composing several days of POLDER measurements. In this paper, POLDER level-2 “ERB & clouds” products (Buriel et al., 1997) are considered. They provide cloud properties (cloud fraction, optical depth, pressure, phase, etc.) and radiances in all viewing directions averaged over $\approx 56 \times 56$ km² “super-pixel” regions ($\approx 9 \times 9$ full-resolution 6×6 km² POLDER pixels).

3. The multi-polarization capability of POLDER

The most original characteristics of POLDER is its ability to measure the polarized component of the Earth-atmosphere reflected light. It allows for determining two important cloud parameters, namely the

cloud thermodynamic phase and the Rayleigh cloud pressure (this later parameter is not discussed here; for details see Goloub et al., 1994; Parol et al., 1999).

Theoretical as well as experimental studies have shown that polarized signatures of water droplets and ice particles are quite different (Goloub et al., 1994; Sauvage et al., 1999; Chepfer et al., 1999). Considering a cloudy system observed from satellite, the polarized component of the upward radiance is mainly formed in the upper cloud layer. Around 80% of the single-scattered radiation reflected by the cloud arises from the upper hundred meters of the layer. Thus, the polarization features mainly governed by single scattering are preserved in the polarized reflectance. For optical thickness large enough, the polarized reflectance roughly varies as the cloud polarized phase function, which depends on cloud microphysics properties (shape/size) and refractive index.

Figs. 1(a)–(b) present respectively, theoretical simulations and observations of the main polarization features for the scattering angle range sampled by POLDER. The light scattered by cloud water droplets exhibits a strong maximum about 140° from the incoming direction. This peak, the so-called primary rainbow, is highly polarized which makes it easily detectable. The maximum and the width of the peak depend on the droplet size distribution (Goloub et al., 1994). Another noticeable property is the zero polarization for scattering angles between 75° and 120° according to droplet size distribution. Finally, for narrow droplet size distributions, several supernumary bows appear beyond 150° (Goloub et al., 1997). On the contrary, for broad size distributions, the phase function maxima and minima are smoothed out. If the droplet size distribution is relatively narrow, Bréon and Goloub (1998) have shown that the supernumary bows can be used to infer the effective radius of liquid water droplets. However, their method only probes a cloud layer of optical thickness less than about 1 located at the cloud top. As illustrated in Fig. 2, applying their inversion method to the full ADEOS 1-POLDER dataset provides global maps of cloud top droplet effective radius estimate (Bréon and Colzy, 2000).

Unlike water clouds, cirrus clouds are mainly composed of ice crystals with extremely large variabilities in shape and size (Krupp, 1991; Miloshevich and Heymsfield, 1997). Diversity and complexity of ice crystal shape and size depend on temperature and humidity in cloud. For scattering angles sampled by POLDER, radiative transfer computations performed for randomly oriented ice particles (Fig. 1(a)) and observations (Fig. 1(b)) show different important features: (i) a generally positive polarization (vibration perpendicular to the scattering plane), (ii) a decreasing of the polarization for increasing scattering angles (i.e., negative slope), (iii) a neutral point around 160° .

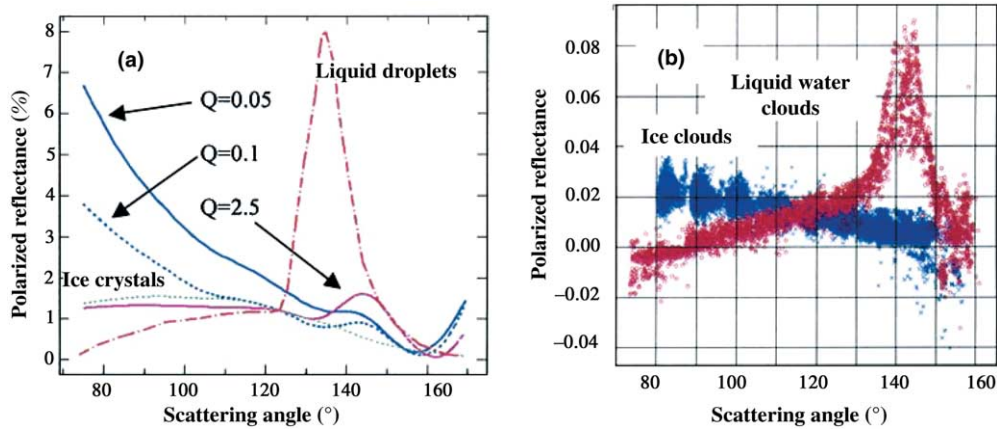


Fig. 1. Polarized reflectance at 865 nm as a function of scattering angle. (a) Corresponds to simulation in the solar principal plane with different ice crystal shapes and one liquid water droplet model (red dashed line) for an optical thickness of 2. Green dots correspond to polycrystals randomly oriented in space (Macke et al., 1996). The other curves correspond to hexagonal particles with different aspect ratio $Q = L/2R$, where L and R are the length and the radius of the particle, respectively. (b) An example of polarized reflectance measured by ADEOS 1-POLDER over cirrus clouds (in blue) and over liquid water clouds (in red). Polarization signatures of liquid and ice clouds display significantly different features that allow for simple and direct cloud thermodynamic phase discrimination.

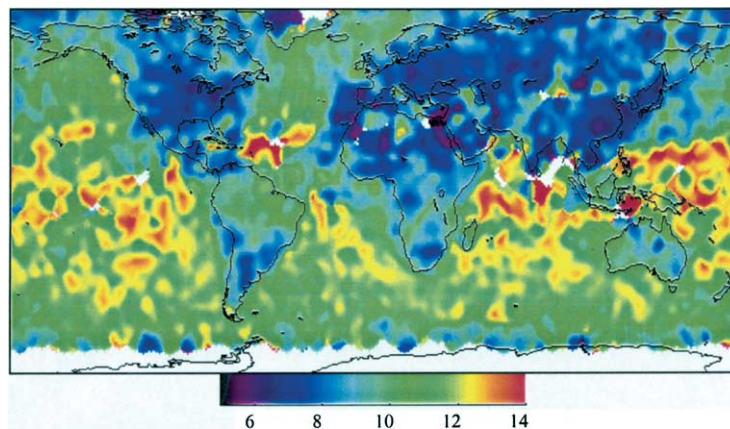


Fig. 2. Seasonal composite of droplet effective radius of liquid water clouds for the March 97–May 97 period at 2.5° resolution. The effective radius values vary from 5 to 14 μm from dark violet to red. This map clearly highlights the land/ocean contrast with droplets smaller over continents than over oceans. (Adapted from Bréon and Colzy, 2000.)

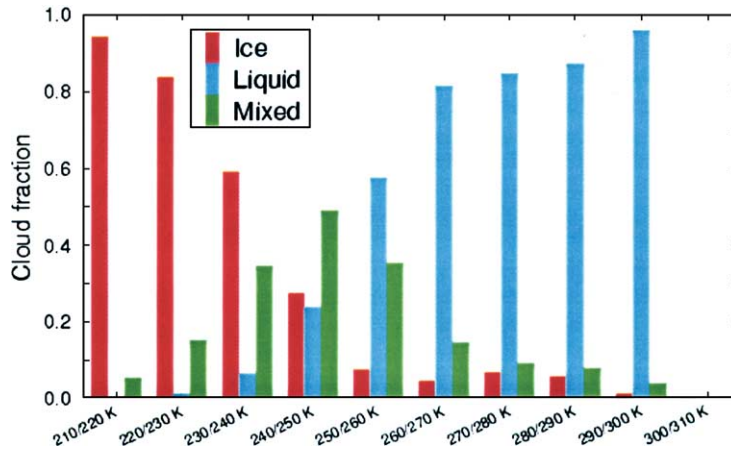


Fig. 3. Cloud cover distribution as a function of cloud temperature. Cloud phase and pressure are derived from POLDER polarization measurements. Temperature is then derived from pressure by using meteorological profile. (Adapted from Doutriaux-Boucher et al., 2002.)

Accounting for these different angular behaviors, the ADEOS 1-POLDER operational algorithm derives the cloud thermodynamic phase. Studies involving global database such as ISCCP (International Cloud Climatology Project) data (Rossow and Schiffer, 1999) and ground-based active remote sensors at the Atmospheric Radiation Measurements Southern Great Plains (ARM-SGP) site (Clothiaux et al., 2000) have shown the high quality of the POLDER phase recognition scheme (Riedi et al., 2000, 2001). Comparison undertaken with Lidar network data is also very informative (Chepfer et al., 2000).

The “ERB & clouds” derived cloud parameters can be very informative for testing some cloud parameterizations involved in climate models. For instance, cloud phase is a very important parameter for cloud study and it needs to be properly parameterized in both climate and mesoscale models. In some of them, the liquid/solid cloud fraction in a grid mesh is defined as a very crude function of the temperature. As illustrated in Fig. 3, combination of temperature profiles and POLDER cloud phase results allows for testing such parameterizations.

4. The multi-directionality capability of POLDER

In Section 3, it clearly appears that the multi-angle capability is necessary for taking advantage of polarization. In addition, the multi-directionality of POLDER is also useful for deriving cloud properties. This multi-directional capability is used in the cloud detection algorithm of the “ERB & clouds” line (Buriel et al., 1997; Sèze et al., 1999). A series of sequential tests are applied to each pixel and for every viewing direction. As an example, over ocean a simple reflectance threshold test can always be applied since a POLDER pixel can be observed with angular configuration outside the sunlight region.

More interestingly, the multi-directional capability of POLDER allows for checking schemes of cloud optical thickness retrieval. Cloud optical thickness is directly related to the ice/liquid water content and is thus a key parameter in cloud modeling. It can be derived from bidirectional reflectance measurements. However, some assumptions about cloud microphysics, cloud morphology and the spatial distribution of clouds are needed in order to infer cloud optical thickness from satellite measurements. Cloud fields are commonly viewed as a single and homogeneous plane-parallel layer composed of prescribed particles despite possibly large effects due to both cloud heterogeneities (Loeb and Coakley, 1998) and different particles (Mishchenko et al., 1996). Unlike the usual scanner radiometers, POLDER provides up to 14 quasi-simultaneous reflectance measurements of a geographical target. While it is always possible to find a cloud model that satisfies one

single bidirectional observation of a given target, it is not so easy to fulfill the complete set of 14 observations. Consequently, POLDER not only allows determining cloud optical thickness under some hypotheses, but it also enables us to test the validity of these hypotheses.

A cloud water droplet model is used in the algorithm that operationally derived cloud optical thickness from ADEOS 1-POLDER data. The cloudy pixels are assumed fully covered by a plane-parallel layer composed of liquid water droplets with an effective radius of $10\ \mu\text{m}$ and an effective variance of 0.15. In these conditions, the optical thickness is the only cloud property that is allowed to vary. The purpose here is to illustrate the ability to test the cloud model used. To do that, for the cloudy situations observed over ocean during three ADEOS overpasses, the N (<14) “directional” values of cloud optical thickness are used. Since the retrieval is based on the standard cloud droplet model, these N values are expected to be close to one other in the case of liquid water clouds and dispersed in the case of ice clouds. The thermodynamic phase is identified for the cloudy pixels as noted in Section 3. We thus select the super-pixels (composed of 9×9 POLDER pixels) for which the phase is found liquid and the super-pixels for which the phase is ice whatever the pixel. For every super-pixel observed from at least seven directions, we calculate the difference between each of the “directional” values of optical thickness and their mean value. More precisely, we use a representation, introduced in the ISCCP (Rossow and Schiffer, 1991) scheme, that is equivalent in radiative energy amount. Indeed, the variability of the cloud properties we are interested in, is important according to their contribution to the ERB. Practically, the calculated parameter is the cloud spherical (or diffuse) albedo defined for a plane-parallel cloud layer over a black surface with no atmosphere. It is obtained by integrating the reflectance over all viewing zenith, solar zenith and relative azimuth angles. Therefore it is a one-to-one function of the optical thickness for a given microphysical model.

The difference between the directional and the directionally-averaged cloud spherical albedo is reported as a function of scattering angle for the super-pixels classified as liquid water clouds in Fig. 4(a). On average, the liquid water clouds appear well represented by the standard droplet model (effective radius of $10\ \mu\text{m}$). Ideally, the spherical albedo difference should be zero. It is typically 0.014 (the mean relative albedo difference is 2.8%). It remains close to zero for the scattering angles larger than 90° . The values of scattering angle around 80° correspond to large solar zenith angles in the forward direction, which may induce a serious weakness of the plane-parallel approximation as already noted from AVRRR (advanced very high resolution radiometer) observations (Loeb and Coakley, 1998). We will come back to this point later.

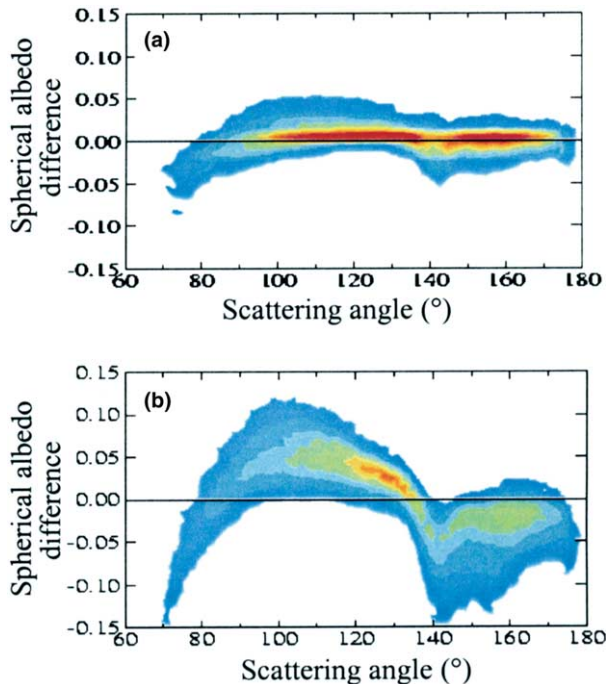


Fig. 4. Difference between the directional and the directionally averaged cloud spherical albedo as a function of scattering angle, (a) for liquid water clouds and (b) for ice clouds. These cloud spherical albedo values are derived from POLDER reflectance measurements at 670 nm by using the standard droplet model (effective radius of 10 μm). Results correspond to overcast conditions over ocean for November 10, 1996. The rainbow color scale represents the density of the measurements, from low density (in blue) to high density (in red). (Adapted from Doutriaux-Boucher et al., 2000.)

4.1. Multidirectional observations over ice clouds

The cloud spherical albedo difference calculated for the super-pixels classified as ice clouds is reported in Fig. 4(b). As expected, it clearly appears that the liquid water droplet model is not suitable for ice clouds. The difference of retrieved spherical albedo is typically 0.045 (10% in relative difference), that is three times larger than in the case of liquid water clouds. It often reaches values as large as ± 0.1 . The minimum observed near 140° is related to the peak of the phase function of the water droplet model in the rainbow direction. It clearly appears that a smoother phase function would give a better agreement in the treatment of ice clouds.

Many studies have shown that the single-scattering properties of ice cloud particles differ substantially from those of liquid water spheres (see Mishchenko et al., 1996 and references therein). For that reason, an ice fractal polycrystal model (Macke et al., 1996), which is expected to be representative of irregularly shaped and randomly oriented ice particles, was introduced in the treatment of cold clouds in the ISCCP re-analysis (Rossow and Schiffer, 1999). Re-analysis of ADEOS1-POLDER data confirmed that some ice crystal models are more adequate for cirrus clouds because they mini-

mize the angular variability of the cloud spherical albedo (Doutriaux-Boucher et al., 2000; C.-Labonnote et al., 2000). For overcast situations over ocean, the cloud spherical albedo RMS difference is 0.031 (6.5%) with the polycrystal model (instead of 0.045 (10%) with the droplet model). However better results are obtained by using an inhomogeneous hexagonal monocrystal (IHM) model, which gives a cloud spherical albedo RMS difference of only 0.016 (mean relative difference of 3.3%). The IHM model corresponds to randomly oriented hexagonal ice crystals containing spherical air bubbles. Air bubble inclusion appears very often inside cirrus ice particles due to a rapid growing of crystals. This model follows some in situ measurements performed from ice replicator and microphotographic observations (Strauss et al., 1997). The IHM model gives results that notably differs from those obtained with a pure hexagonal monocrystal (PHM) model, i.e., without air bubbles, as reported in Fig. 5. The PHM model gives

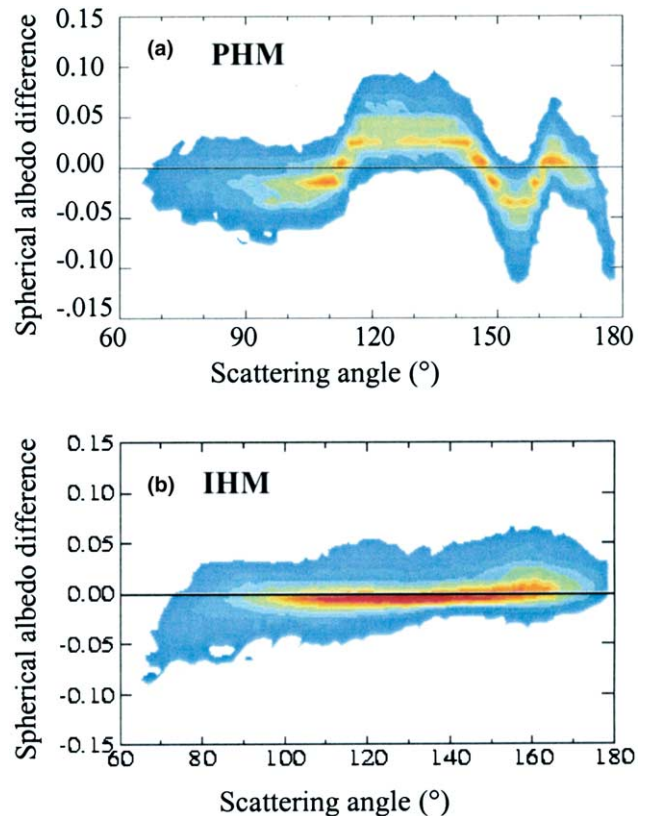


Fig. 5. Difference between the directional and the directionally-averaged cloud spherical albedo as a function of scattering angle for ice clouds. These cloud spherical albedo values are derived from POLDER reflectance measurements at 670 nm, (a) by using the PHM model and (b) by using the IHM model. The two models correspond to the same hexagonal ice crystal with an aspect ratio $L/2R = 220 \mu\text{m}/44 \mu\text{m}$ but without and with air bubble inclusions, respectively. Results correspond to overcast ice clouds observed on November 10, 1996. The rainbow color scale represents the density of the measurements, from low density (in blue) to high density (in red). (Adapted from C.-Labonnote et al., 2000.)

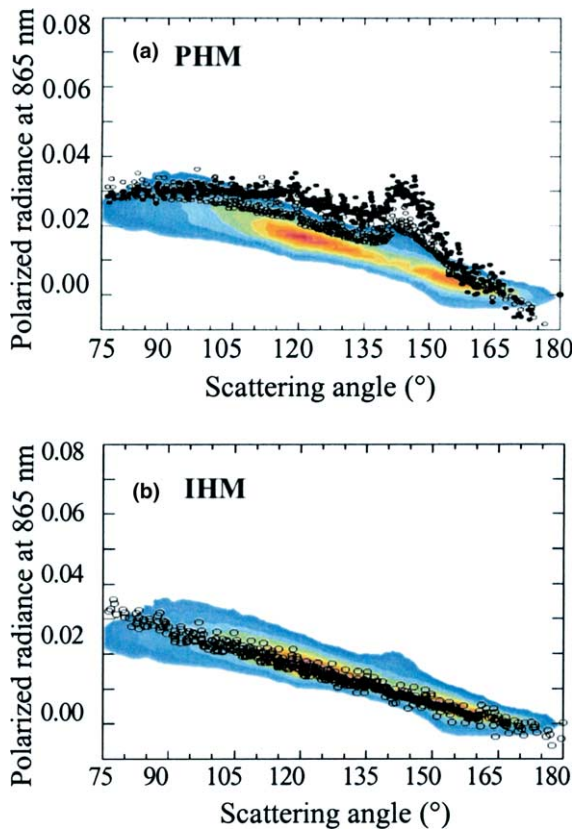


Fig. 6. Comparison between the ADEOS 1-POLDER observations of polarized radiance at 865 nm and the two ice crystal models of Fig. 4. Results correspond to overcast ice clouds over ocean. The rainbow color scale represents the density of the measurements, from low density (in blue) to high density (in red). The small circles correspond to simulations. (Adapted from C.-Labonnote et al., 2001.)

a cloud spherical albedo RMS difference of 0.029 and a mean relative difference almost twice larger than the IHM model. Note that this clear superiority of the IHM model is also observed in the polarization measurements as reported in Fig. 6. This model has been retained for the operational processing of the ADEOS 2-POLDER data (launched in December 2002).

4.2. *Multidirectional observations over liquid water clouds*

Now let us come back to the liquid water clouds. They are rather well represented by the standard droplet model as already shown in Fig. 4(a). However, significant differences between model and observations appear in the rainbow direction ($\theta \sim 140^\circ$) and for the smallest observable values of scattering angle ($\theta < 90^\circ$). To go further, we examine the difference $S(\theta) - S(120^\circ)$ between the directional value of cloud spherical albedo in the θ -direction and its value at the reference scattering angle of 120° . This difference averaged over a lot of observations sampled throughout the eight months of available ADEOS 1-POLDER data is reported in Fig. 7. The difference $S(\theta) - S(120^\circ)$ is consistent with the difference between $S(\theta)$ and the directionally averaged value reported in Fig. 4(a).

Cloud spherical albedos retrieved with the standard droplet model are too small in the rainbow direction. That suggest that the cloud particle size is too large in the model. The cloud spherical albedo difference $S(\theta) - S(120^\circ)$ retrieved by using a cloud particle distribution with an effective radius of $5 \mu\text{m}$ (instead of

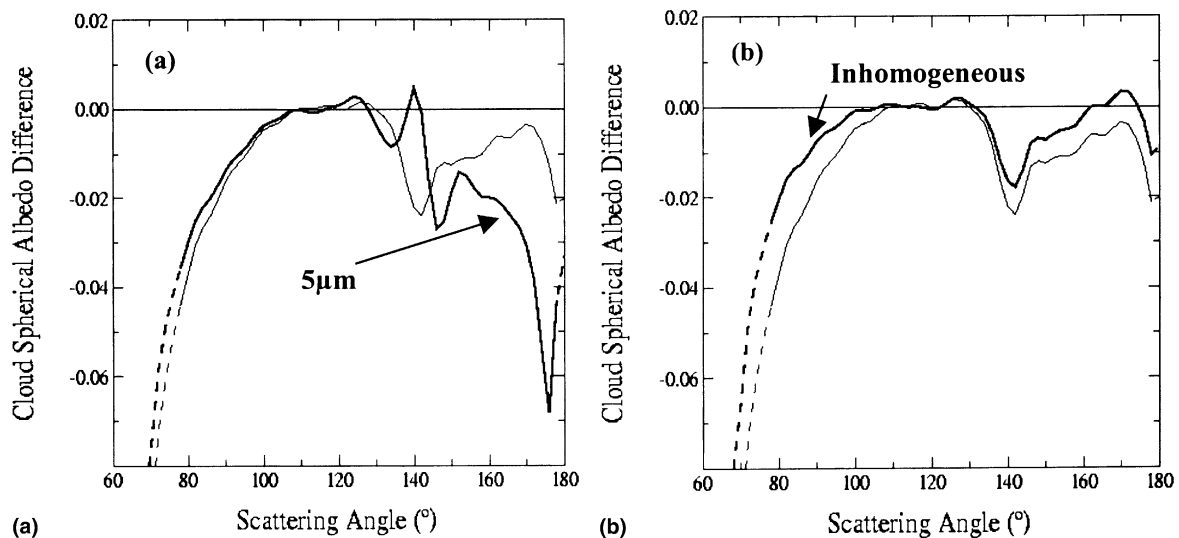


Fig. 7. Difference between the directional values of cloud spherical albedo and the reference value at 120° as a function of scattering angle. Results are derived from ADEOS 1-POLDER observations at 670 nm in the case of overcast liquid water clouds over ocean. The thin lines corresponds to the homogeneous cloud droplet model with an effective radius of $10 \mu\text{m}$. On the left, the thick lines correspond to the $5 \mu\text{m}$ model. On the right, they correspond to the inhomogeneous cloud model. In both cases, the full lines correspond to precise mean differences. (Adapted from Buriez et al., 2001.)

10 μm) is reported in Fig. 7(a). As expected, the 5- μm model is more suitable than the 10- μm model for scattering angles very close to 140° . However, it is hardly more convenient for small scattering angles and quite less adequate for scattering angles beyond 150° . Practically, any realistic microphysics of liquid water cloud is insufficient to explain the decrease of the retrieved cloud spherical albedo in the forward direction ($\Theta < 90^\circ$).

Spatial variations in cloud optical thickness can also have a large impact on cloud property retrievals. The cloud spherical difference $S(\Theta) - S(120^\circ)$ retrieved by using a horizontally inhomogeneous cloud model is reported in Fig. 7(b). To do that, we use the gamma independent pixel approximation of Barker et al. (1996) with a standard deviation of the cloud optical distribution as large as the mean at the pixel scale. Despite the high degree of horizontal heterogeneity of the considered model, we observe only a very weak improvement compared to the homogeneous cloud layer model. Our feeling is that the major deficiency is chiefly due to subpixel-scale variations in cloud top height (i.e., cloud bumps). A similar conclusion was obtained from theory by Loeb and Coakley (1998), who argued that cloud top variability is responsible for the marked angular dependence in plane-parallel errors, particularly for large solar zenith angles in the forward-scattering direction.

5. The multispectral capability of POLDER

The instrumental concept of POLDER is based on a rotating wheel carrying spectral filters of which central wavelengths range between 443 and 910 nm. Comparing to previous multispectral radiometers, a novel contribution of POLDER is the use of a differential absorption technique for estimating the mean cloud pressure.

An apparent pressure P_{app} is derived from O_2 -absorption measurements at 763 nm assuming a non-

scattering atmosphere. Because all the scattering effects are neglected, Vanbauce et al. (1998) have shown that the measured difference between P_{app} and the cloud top pressure derived from thermal infrared measurements is on an average of the order of 180 hPa for optically thick clouds. More recently, comparisons of lidar and radar measurements from the ARM-SGP site make P_{app} appears closer to the mean cloud pressure than to the cloud top pressure (Vanbauce et al., 2003). However, the difference between P_{app} and the cloud mean pressure can be amplified when the ground influence is important, i.e., over land. This problem practically disappears using a simple surface correction as well as an optical thickness filter that reduces the errors in retrieval due to the cloud semi-transparency. Even if the corrected cloud pressure remains far away from the cloud top pressure (125 hPa on average), it is now very close to the mean pressure whatever the cloud type is (Vanbauce et al., 2003).

The last important point developed in this paper is the derivation of the shortwave (SW) albedo using the multispectral capability of the POLDER instrument. It is of prime interest for climate study to estimate the SW cloud forcing. This parameter is directly related to the difference between the actual observed SW albedo and its clear-sky estimate. In the POLDER “ERB & clouds” operational algorithm, the SW albedo is derived as a function of the three spectral albedos at 443, 670 and 865 nm. It is worthy of note that, thanks to its multi-angle observations, POLDER obtains direct information on the anisotropy of the reflected radiation field (see Section 4). Thus, for each scene, the spectral albedos are computed as angle-weighting averages of the 14 different angular values derived using the same plane-parallel model as for the derivation of cloud optical thickness. The SW albedo derivation takes into account the atmospheric absorption, in particular the solar water vapor absorption estimated from the ratio of the POLDER reflectances at 865 and 910 nm.

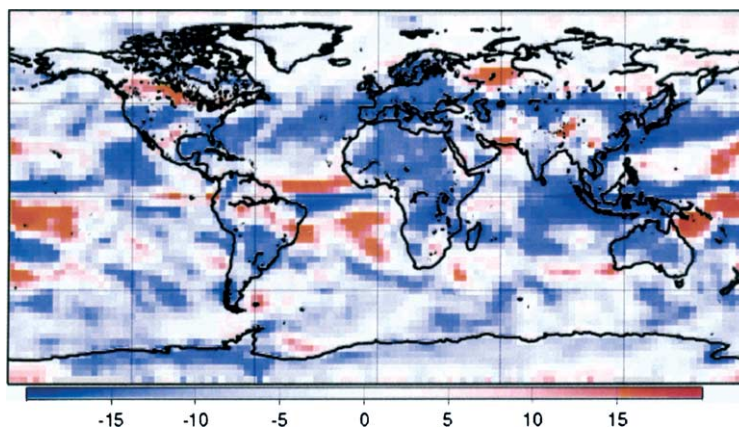


Fig. 8. Shortwave reflected flux anomaly (W m^{-2}) for March 1997 referenced to the 1985–1989 ERBE monthly means. This map corresponds to $2.5^\circ \times 2.5^\circ$ gridded values. The large blue areas indicate POLDER flux lower than ERBE one. Unusual features are observed over the western Pacific (in red) where the convection is enhanced whereas large parts of Indonesia are cloud-free (in blue). This corresponds to the beginning of the 1997–1998 ENSO warm event. (Adapted from Viollier et al., 2002.)

The SW albedo which is an instantaneous albedo at the local time of observation (around 10:30 UTC for ADEOS 1-POLDER) is generally not equivalent to the daily average. For this reason, a diurnal interpolation and extrapolation procedure is applied to the POLDER result, by adjusting algorithms previously developed for ScaRaB (Standfuss et al., 2001). The daily and monthly means of the reflected SW fluxes at the top of the atmosphere are then deduced. Since the ADEOS 1-POLDER period corresponds to the beginning of the 1997–1998 ENSO warm event, the monthly maps of POLDER SW flux reveal strong deviations in the Tropical Pacific, as illustrated in Fig. 8. On the other hand, on average, the POLDER 20S–20N reflected solar flux is smaller by about 2.7 and 7 W m^{-2} when compared to CERES/Terra and 1985–1989 ERBE results for a mean value of 90 W m^{-2} (Viollier et al., 2002). This reasonable discrepancy (3–7%) between POLDER and the ERB instruments may be partly due to the uncertainties in the POLDER calibration and to the narrowband to broadband extrapolation procedure. More accurate comparisons using simultaneous observations of ADEOS 2-POLDER and CERES/Terra should make this point clearer.

6. Conclusion

This paper emphasizes the original capabilities of POLDER for cloud parameter retrievals. As the usual operational algorithms that furnish satellite derived cloud parameters, the POLDER ‘ERB & Clouds’ processing line provides some ‘standard’ cloud properties like cloud fraction and cloud optical depth at global scale. Moreover, novel cloud and atmospheric parameters are also inferred from the three original characteristics of POLDER. A cloud phase index and two cloud pressures are currently distributed on a daily (level-2 product) and a monthly (level-3 product) basis by the CNES in Toulouse, France.

As illustrated in this paper, the multi-polarization capability of POLDER combined with the multi-directionality of the instrument allow for inferring the cloud thermodynamic phase and the effective radius of liquid water droplets at global scale. On the other hand, the multi-directionality of POLDER allows for checking schemes of cloud optical thickness and cloud albedo retrieval. Usual assumptions both on cloud microphysics (spherical particles) and on cloud morphology (homogeneous plane-parallel layer) have been tested. The mean observed angular variability of cirrus reflectances is shown to be better represented by using an IHM model than a cloud water droplet model. Comparisons between POLDER measurements and simulations of cirrus cloud polarization confirm the relevance of the IHM model.

In the ‘ERB & Clouds’ operational algorithm, liquid water clouds are assumed to be plane-parallel layers composed of droplets with an effective radius of 10 μm . However, the angular variabilities of reflectances for liquid water clouds show significant differences between model and observations in the rainbow direction and for the smallest observable values of scattering angle. Changing the water droplet size distribution does not lead to a significant improvement except in the rainbow direction. On the other hand, the introduction of a high degree of horizontal heterogeneity at the sub-pixel pixel leads only to a weak improvement. The major deficiency of the plane-parallel model seems to be due to cloud top height variations which are not taken into account.

The multispectral capability of POLDER allows for estimating the mean cloud pressure from O_2 -absorption measurements at 763 nm. Comparisons with cloud pressure derived from lidar and radar measurements from the ARM-SGP site show a very good agreement. The last important point developed in this paper is the derivation of the SW flux using the multispectral capability of POLDER. It is shown that global maps of POLDER albedo reveal strong deviations in the Tropical Pacific, that correspond to the beginning of the 1997–1998 ENSO event. On the other hand, when compared to the CERES/Terra and ERBE results, the monthly mean of the POLDER 20S–20N reflected SW flux is smaller by about 2.7 and 7 W m^{-2} , respectively, for a mean value of 90 W m^{-2} . More accurate comparison using simultaneous observations of ADEOS 2-POLDER and CERES/Terra are planned in the next months and should make this point clearer.

The 8-months POLDER cloud dataset allows to build a cloud climatology including original property like cloud thermodynamic phase. Preliminary comparisons between POLDER and ISCCP monthly mean products (cloud cover, cloud optical thickness, and cloud pressure) outline some differences resulting for a part from the original characteristics (multidirectionality and multipolarization) of POLDER (Parol et al., 1999). POLDER aboard the ADEOS 2 platform will permit to go further in this way. The ADEOS 2 satellite has been successfully launched on December 14, 2002. The first POLDER test image was acquired over France on February 1, 2003 and ADEOS 2-POLDER continuous data acquisition started in April 2003. Advanced algorithms have been developed for POLDER 2 data, from the analysis of POLDER 1 results. Comprehensive information and preliminary results are presented on the POLDER web site <http://smc.cnes.fr/POLDER/>.

Acknowledgements

This study was funded by CNES, EEC, Région Nord-Pas de Calais, and Préfecture du Nord through EFRO.

Currently updated information about POLDER project is available from <http://smc.cnes.fr/POLDER/>.

References

- Barker, H.W., Wielicki, B.A., Parker, L. A parameterization for computing grid-averaged solar fluxes for inhomogeneous marine boundary layer clouds. Part II: validation using satellite data. *J. Atmos. Sci.* 53, 2304–2316, 1996.
- Barkstrom, B.R., Harrison, E.F., Smith, G.L., Green, R., Kibler, J., Cess, R., and the ERBE Science Team. Earth radiation budget experiment (ERBE) archival and April 1985 results. *Bull. Amer. Meteor. Soc.* 70, 1254–1262, 1989.
- Buriez, J.C., Vanbauce, C., Parol, F., et al. Cloud detection and derivation of cloud properties from POLDER. *Int. J. Remote Sens.* 18, 2785–2813, 1997.
- Buriez, J.C., Doutriaux-Boucher, M., Parol, F., Loeb, N.G. Angular variability of the liquid water cloud optical thickness retrieved from ADEOS-POLDER. *J. Atmos. Sci.* 58, 3007–3018, 2001.
- Bréon, F.M., Goloub, P. Cloud droplet effective radius from spaceborne polarization measurements. *Geophys. Res. Lett.* 25, 1879–1882, 1998.
- Bréon, F.M., Colzy, S. Global distribution of cloud droplet effective radius from POLDER polarization measurements. *Geophys. Res. Lett.* 27, 4065–4068, 2000.
- Chepfer, H., Brogniez, G., Sauvage, L., et al. Remote sensing of cirrus radiative parameters during EUCREX'94. Case study of 17 April 1994. Part II: Microphysical modelization. *Mon. Wea. Rev.* 127, 504–518, 1999.
- Chepfer, H., Goloub, P., Spinhirne, J., et al. Cirrus cloud properties derived from POLDER-1/ADEOS polarized radiances: first validation using a ground-based Lidar network. *J. Appl. Meteor.* 39, 154–168, 2000.
- C.-Labonnote, L., Brogniez, G., Gayet, J.F., Doutriaux-Boucher, M., Buriez, J.C. Modeling of light scattering in cirrus clouds with inhomogeneous hexagonal monocrystals. Comparison with in situ and ADEOS-POLDER measurements. *Geophys. Res. Lett.* 27, 113–116, 2000.
- C.-Labonnote, L., Brogniez, G., Buriez, J.C., et al. Polarised light scattering by inhomogeneous hexagonal monocrystals. Validation with ADEOS-POLDER measurements. *J. Geophys. Res.* 106, 12,139–12,153, 2001.
- Clothiaux, E.E., Ackerman, T.P., Mace, G.G., et al. Objective determination of cloud heights and radar reflectivities using a combination of active remote sensors at the ARM CART sites. *J. Appl. Meteor.* 39, 645–665, 2000.
- Doutriaux-Boucher, M., Buriez, J.C., Brogniez, G., et al. Sensitivity of retrieved POLDER directional cloud optical thickness to various ice particle models. *Geophys. Res. Lett.* 27, 109–112, 2000.
- Doutriaux-Boucher, M., Quaas, J., Giraud, V., Sèze, G., Vanbauce, C. Comparison of Cloud/Phase/Temperature relationships in the LMD GCM and POLDER/METEOSAT data. Eumetsat satellite Conference, Dublin, Ireland, 2–6 September 2002.
- Goloub, P., Deuzé, J.-L., Herman, M., Fouquart, Y. Analysis of the POLDER polarization measurements performed over cloud covers. *IEEE Trans. Geosci. Rem. Sens.* 32, 78–88, 1994.
- Goloub, P., Chepfer, H., Herman, M., et al. Use of polarization for clouds study. *Proc. SPIE's* 1997 3121, 330–341, 1997.
- Kandel, R., Viollier, M., Raberanto, P., et al., and the International ScaRaB Scientific Working Group (ISSWG). The ScaRaB Earth Radiation Budget Dataset. *Bull. Amer. Meteor. Soc.* 79, 765–783, 1998.
- Krupp, C. Holographic measurements of ice crystals in cirrus clouds during the International Cirrus Experiment ICE. in: Saunders, R.W., Brown, P.R.A., (Eds.), Report of the 4th ICE/EUCREX Workshop. available from Meteorological Research Flight pp. 58–67, 1991.
- Loeb, N.G., Coakley, J.A. Inference of marine stratus cloud optical depths from satellite measurements: Does ID theory apply? *J. Climate* 11, 215–233, 1998.
- Macke, A., Mueller, J., Raschke, E. Single scattering properties of atmospheric ice crystals. *J. Atmos. Sci.* 53, 2813–2825, 1996.
- Miloshevich, L.M., Heymsfield, A.J. A balloon-borne continuous cloud particle replicator for measuring vertical profiles of cloud microphysical properties: Instrument design, performance, and collection efficiency analysis. *J. Atmos. Oceanic. Technol.* 14, 753–768, 1997.
- Mishchenko, M.I., Rossow, W.B., Macke, A., Lacis, A.A. Sensitivity of cirrus cloud albedo, bidirectional reflectance and optical thickness retrieval accuracy to ice particle shape. *J. Geophys. Res.* 101, 16,973–16,985, 1996.
- Parol, F., Buriez, J.C., Vanbauce, C., et al. First results of the POLDER “Earth Radiation Budget and Clouds” operational algorithm. *IEEE Trans. Geosci. Rem. Sens.* 37, 1597–1612, 1999.
- Riedi, J., Doutriaux-Boucher, M., Goloub, P., Convert, P. Global distribution of cloud top phase from POLDER/ADEOS 1. *Geophys. Res. Lett.* 27, 1707–1710, 2000.
- Riedi, J., Goloub, P., Marchand, R. Comparison of POLDER phase retrievals to active remote sensors measurements at the ARM SGP site. *Geophys. Res. Lett.* 28, 2185–2188, 2001.
- Rossow, W.B., Schiffer, R.A. ISCCP cloud data products. *Bull. Amer. Meteor. Soc.* 72, 2–20, 1991.
- Rossow, W.B., Schiffer, R.A. Advances in understanding clouds from ISCCP. *Bull. Amer. Meteor. Soc.* 80, 2261–2287, 1999.
- Sauvage, L., Chepfer, H., Trouillet, V., et al. Remote sensing of cirrus radiative parameters during EUCREX'94. Case study of 17 april 1994. Part I: Observations. *Mon. Wea. Rev.* 127, 486–503, 1999.
- Sèze, G., Vaubauce, C., Buriez, J.C., et al. Cloud cover observed simultaneously from POLDER and METEOSAT. *Phys. Chem. Earth* 24, 921–926, 1999.
- Standfuss, C., Viollier, M., Kandel, R.S., Duvel, J.Ph. Regional diurnal albedo climatology and diurnal time extrapolation of reflected solar flux observations, Application to the ScaRaB record. *J. Climate* 14, 1129–1146, 2001.
- Strauss, B., Meerkoetter, R., Wissinger, B., Wendling, P., Hess, M. On the regional climatic impact of contrails: microphysical and radiative properties of contrails and cirrus. *Annales Geophys.* 15, 1457–1467, 1997.
- Vanbauce, C., Buriez, J.C., Parol, F., Bonnel, B., Sèze, G., Couvert, P. Apparent pressure derived from ADEOS-POLDER observations in the oxygen A-band over ocean. *Geophys. Res. Lett.* 25, 3159–3162, 1998.
- Vanbauce, C., Cadet, B., Marchand, R.T. Comparison of POLDER apparent and corrected oxygen pressure to ARM/MMCR cloud boundary pressures. *Geophys. Res. Lett.* 30 (5), 1212, 2003.
- Viollier, M., Standfuss, C., Parol, F. Monthly means of reflected solar flux from POLDER(ADEOS-1) and comparison with ERBE, ScaRaB and CERES. *Geophys. Res. Lett.* 29, 141-1-4, 2002.
- Wielicki, B.A., Barkstrom, B.R., Harrison, E.F., Lee III, R.B., Smith, G.L., Cooper, J.E. Clouds and the Earth's radiant energy system (CERES): an Earth observing system experiment. *Bull. Amer. Meteor. Soc.* 77, 853–868, 1996.